Biochemical and Biophysical Research Communications 452 (2014) 560–566

Contents lists available at ScienceDirect

Biochemical and Biophysical Research Communications

journal homepage: www.elsevier.com/locate/ybbrc

Altered expression of dopamine receptors in cholinergic motoneurons of the hypoglossal nucleus in a 6-OHDA-induced Parkinson's disease rat model

Li Zhou [a], Zhi-Yong Wang [a], Hui Lian [a], Hai-Yan Song [a], Yi-Min Zhang [a], Xiao-Li Zhang [b], Rui-Fang Fan [b], Li-Fei Zheng [b], Jin-Xia Zhu [a,b,*]

[a] Key Laboratory for Medical Tissue Regeneration of Henan Province, School of Basic Medical Sciences, Xinxiang Medical University, Xinxiang 453003, China
[b] Department of Physiology and Pathophysiology, School of Basic Medical Sciences, Capital Medical University, Beijing 100069, China

ARTICLE INFO

Article history:
Received 14 August 2014
Available online 27 August 2014

Keywords:
Choline acetyltransferase
Tyrosine hydroxylase
Dopamine receptor
Hypoglossal nucleus
6-OHDA

ABSTRACT

Parkinson's disease (PD) is a common neurodegenerative disorder that is often associated with weak tongue motility. However, the link between the degenerated dopaminergic neurons in the substantia nigra (SN) and lingual dysfunction remains unclear. In the present study, we investigated the localization of dopamine receptor 1 (D1) and dopamine receptor 2 (D2) and alternations in their expression in cholinergic motoneurons of the hypoglossal nucleus (HN) using double-label immunofluorescence, Western blotting and semi-quantitative reverse transcription and polymerase chain reaction (SqRT–PCR) in rats that received microinjections of 6-hydroxydopamine bilaterally into the SN (6-OHDA rats). The results revealed that a large population of choline acetyltransferase immunoreactive (ChAT-IR) neurons was distributed throughout HN and that almost all of the ChAT-IR motoneurons were also D1-IR and D2-IR. Several tyrosine hydroxylase (TH)-IR profiles were observed in a nonuniform pattern near the ChAT-IR, D1-IR or D2-IR somas, suggesting potent dopaminergic innervation. In the 6-OHDA rats, TH immunoreactivity in the SN was significantly decreased, but food residue was increased and treadmill occupancy time was shortened. In the HN, protein expression of TH and D2 was increased, whereas that of ChAT and D1 was decreased. A similar pattern was observed in mRNA levels. The present study suggests that dopamine may modulate the activity of cholinergic neurons via binding with D1 and D2 in the HN. Changes in the expression of ChAT, TH, D1 and D2 in the HN of 6-OHDA rats might be associated with the impaired tongue motility in PD. These findings should be further investigated.

1. Introduction

Parkinson's disease (PD) is a common and disabling neurodegenerative disorder that is characterized by a dramatic loss of dopaminergic neurons in the substantia nigra pars compacta (SNpc). Swallowing impairment (dysphagia) is a frequent and often unrecognized complication in patients with PD. The prevalence of dysphagia in patients with PD has been reported to range from 50% to 100%, and this symptom is generally unresponsive to antiparkinson therapy [1,2]. A normal swallowing pattern includes lingual, pharyngeal and esophageal stages. Lingual dysfunction in dysphagia is often present in patients with PD [2], and the most common features include difficulty initiating swallowing, a segmented bolus swallow, prolonged lingual elevation, and subdued tongue movement during bolus propulsion [2–5]. 6-Hydroxydopamine (6-OHDA)-induced PD rats have impaired lingual motor function, which is consistent with deficits observed in patients with PD [6,7].

The hypoglossal nucleus (HN) is composed of cholinergic motoneurons, the axons of which innervate extrinsic and intrinsic muscles of the tongue and control its complex movements through the hypoglossal nerve. The HN is also innervated by noradrenergic [8], dopaminergic [9,10], serotonergic [8], peptidergic [11], and nitrergic fibers [12]. Tyrosine hydroxylase (TH) is the rate-limiting

Abbreviations: PD, Parkinson's disease; SN, substantia nigra; D1, dopamine receptor 1; D2, dopamine receptor 2; HN, hypoglossal nucleus; DMV, dorsal motor nucleus of the vagus; SqRT–PCR, semi-quantitative reverse transcription and polymerase chain reaction; 6-OHDA, 6-hydroxydopamine; ChAT, choline acetyltransferase; IR, immunoreactive; TH, tyrosine hydroxylase; DA, dopamine; NE, noradrenaline; DAPI, 4′,6-diamidino-2-phenylindole.

* Corresponding author at: Key Laboratory for Medical Tissue Regeneration of Henan Province, School of Basic Medical Sciences, Xinxiang Medical University, Xinxiang 453003, China. Fax: +86 373 3831655.
E-mail address: zhu_jx@ccmu.edu.cn (J.-X. Zhu).

http://dx.doi.org/10.1016/j.bbrc.2014.08.104
0006-291X/

enzyme in the biosynthesis of dopamine (DA) and noradrenaline (NE). It is widely distributed throughout the HN [8,13]. In addition, abundant dopamine receptor 1 (D1) mRNA expression has been detected in the HN using *in situ hybridization* [14] and dopamine receptor 2 (D2) binding sites have been observed using autoradiography [15]. However, there is no further morphological evidence available to support dopaminergic regulation of HN motoneuron function. The purpose of the present study was to investigate the distributions of TH-immunoreactive (IR), choline acetyltransferase (ChAT)-IR, and dopamine receptor (DR)-IR in the HN using double-label immunofluorescence as well as to examine their response to 6-OHDA-induced destruction of dopaminergic neurons in the SN by assaying mRNA and protein expression in the HN, which may provide the experimental evidence that elucidates the mechanism underlying the lingual disorder suffered by patients with PD.

2. Materials and methods

2.1. Animals

We used fifty adult male Sprague–Dawley rats (Laboratory Animal Services Center of Capital Medical University, Beijing, China) that ranged in weight from 210 to 250 g. Every procedure was approved by the Animal Care and Use Committee of Capital Medical University and was conducted in accordance with the established guidelines of the National Institutes of Health (NIH, USA). All efforts were made to minimize the number of animals used and their suffering.

2.2. 6-OHDA-treated rat model

The methods employed in the present study have been described previously [16,17]. Briefly, one group of rats ($n = 30$) received bilateral infusions of 6-OHDA (Sigma, St. Louis, MO, USA). After being anesthetized with chloral hydrate (0.4 g/kg), rats were placed on a Kopf stereotaxic instrument. Two areas of the skull were exposed (coordinates: AP, −5.6 mm; ML, ±2.0 mm; DV, −7.5 mm) and 6-OHDA (4 μg in 2 μl of 0.9% saline containing 0.05% ascorbic acid) was injected with a 10 μl Hamilton syringe. A sham control group included 20 rats that were injected with 0.2% ascorbic acid/saline solution. Of the 30 rats treated with 6-OHDA, 16 presented a greater than 60% loss of dopaminergic neurons in the SN and were used for further study.

2.3. Immunohistochemistry

Rats were anesthetized with chloral hydrate (0.4 g/kg) and then perfused with chilled phosphate-buffered saline (PBS 0.1 M), followed by 4% paraformaldehyde (300 ml) in 0.1 M PBS. The brains were then removed and immersed in 4% paraformaldehyde overnight at 4 °C. They were then transferred into graded sucrose and subsequently frozen. Serial frontal sections (20 μm) were cut on a cryostat (Leica CM1850, St. Gallen, Switzerland) through brainstem blocks that contained the HN and then thaw mounted onto glass slides. All slides were stored at −80 °C until further testing.

The sections were brought to room temperature and washed in 0.01 M PBS (pH 7.4). Sections were then permeabilized with 0.3% Triton X-100 and immersed in 10 mM citrate buffer (pH 6.0) to perform microwave antigen retrieval. After blocking nonspecific binding, sections were incubated with a mixture of two primary antibodies overnight at 4 °C (Table 1). Sections were subsequently incubated with a mixture of the two secondary antibodies for 1 h at room temperature. The cell nuclei were stained with 4′,6-diamidino-2-phenylindole (DAPI) before being mounted onto antifade media, and the slides were visualized under a confocal microscope (Olympus, FV1000).

2.4. Control experiments

To document the specificity of our staining, several control experiments were performed following the protocols of a previous study [18]: (I) two or three antibodies for ChAT, D1 and D2 from different companies were used, and the distribution features of the immunoreactive neurons or fibers were identical; (II) slides from the striatum were used as a positive control for TH, D1 and D2 antibodies; (III) a group that did not receive primary antibodies and a preabsorption group were used as negative controls; and (IV) cross-reactivity was not observed between antibody groups during double-label immunofluorescence.

2.5. Tissue preparation for protein and mRNA extraction

The SN and HN were collected on ice from the brains of control and 6-OHDA rats. Animals were sacrificed and decapitated, and the brainstems were quickly removed. The left and right hypoglossal nuclei were dissected on ice according to the protocol published by Yu [19] and then submerged in liquid nitrogen. Tissues were stored at −80 °C until further testing.

2.6. Western blot analysis

Tissues were homogenized in 50 μl of cold lysis buffer supplemented with protease inhibitors for protein extraction (1% Nonidet P-40; 10 mM Tris–HCl, pH 8.0; 5 μg/ml leupeptin; 150 mM NaCl; 1 mM EDTA; 2% SDS; 5 μg/ml aprotinin; 1 mM PMSF; 0.5% deoxycholic acid; and 1 mM sodium orthovanadate, all purchased from Sigma Company). Proteins (25 μg) were separated using a 10% SDS–PAGE gel. Following electrophoresis, proteins were transferred onto a nitrocellulose membrane (NC membrane, Millipore, Billerica, MA, USA) at 4 °C, washed for 10 min in TBST (20 mM Tris–Cl, pH 7.4, containing 0.15 M NaCl, 2.7 mM KCl and 0.05% Tween 20) and blocked for 1 h at room temperature in blocking buffer (10% non-fat dry milk in TBST). The membrane was incubated with primary antibodies in TBST overnight at 4 °C, followed

Table 1
First antibodies used in this study.

Antigen	Antibody	Dilution		Source/catalog no.
		Immunocytochemistry	Western blot	
TH	Mouse monoclonal	1:5000	1:100000	Sigma/T1299
ChAT	Mouse monoclonal	1:50	1:500	Millipore/MAB305
ChAT	Sheep polyclonal	1:50	1:500	Abcam/ab18735
D1	Rabbit polyclonal	1:100	1:500	Abcam/ab20666
D1	Rabbit polyclonal	1:50	1:500	Alomone/ADR-001
D2	Rabbit polyclonal	1:100	1:500	Abcam/ab21218
D2	Rabbit polyclonal	1:50	1:500	Abcam/ab32349
GAPDH	Mouse monoclonal	N/A	1:500	Beyotime/AG019

Table 2
Secondary antibodies used in this study.

Antigen	Conjugation	Dilution	Source/catalog no.
Goat anti-mouse IgG	Alexa Fluor 488	1:1000	Abcam/ab150105
Goat anti-mouse IgG	Alexa Fluor 594	1:1000	Abcam/ab150116
Donkey anti-rabbit IgG	Alexa Fluor 488	1:1000	Abcam/ab150105
Donkey anti-rabbit IgG	Alexa Fluor 594	1:1000	Abcam/ab150076
Donkey anti-sheep IgG	Alexa Fluor 488	1:1000	Abcam/ab150177
Donkey anti-sheep IgG	Alexa Fluor 594	1:1000	Abcam/ab150180
Goat anti-mouse IgG	HRP	1:1000	Beyotime/A0216
Goat anti-rabbit IgG	HRP	1:1000	Beyotime/A0208

by incubation in the appropriate secondary antibodies for 1 h at room temperature (Table 2). The membranes were washed three times (10 min each) in TBST after the antibody incubations. Finally, the blots were scanned using an Odyssey Infrared Imager (LI-COR, Nebraska, USA) and analyzed using Image J (version 1.42, National Institutes of Health, USA), version 1.44.

2.7. RNA extraction and semi-quantitative reverse transcription and polymerase chain reaction (SqRT–PCR)

Total RNA was extracted from the HN using Trizol Reagent (Invitrogen, Carlsbad, CA, USA). A sample of 5 μg of total RNA was used to synthesize the first-strand cDNA using the GoScript Reverse Transcription System (Promega, USA). The RT product was then used as the template to amplify specific fragments. The PCR conditions were individually optimized for each gene studied. Expression of the housekeeping gene β-actin was used as an internal control. The reverse transcription PCR product was separated in a 1.5% agarose gel, and images were scanned using the Bio-best 140M (SIM, USA). The original intensity of each specific band was semi-quantitated using Image J. The data were compared after being normalized to the intensity of β-actin. The sequences of the PCR primers are listed in Table 3.

2.8. Statistical analysis

The values are presented as the means ± S.E.M. (standard error of the mean) from at least three independent experiments; "*n*" refers to the number of animals or tissue samples from different animals. Statistical analysis was conducted using unpaired t-tests. The level of significance was set at $P < 0.05$.

3. Results

3.1. Distribution and expression of ChAT, TH, D1 and D2 in control rats

Antibodies ordered from various companies are listed in Table 1. Double-label immunofluorescence was performed to assess the distribution patterns of ChAT, TH, D1 and D2 in the HN. ChAT-IR neurons (red) were clearly distributed throughout the HN, but appeared abundantly in the caudal half of the HN ventromedially (Fig. 1A/A'). In contrast to the ChAT staining pattern, TH-IR neurons were not observed within the HN, but TH-IR processes associated with varicosities (green) were dispersed in the HN and assumed a relatively high density that was limited to the ventromedial area in the caudal half of the HN (Fig. 1A–C). In the high-resolution images (Fig. 1A'–C'), many TH-IR perisomatic profiles were observed nonuniformly around ChAT-, D1- or D2-IR neurons (empty arrows). According to the topographic distributions of ChAT (Fig. 1A/A' and D/D'), D1 (Fig. 1B/B' and E/E') and D2 (Fig. 1C/C'), several observations were made: (I) D1- and D2-IR neurons were extensively distributed throughout the HN from the rostral to the caudal parts; (II) most of the D1-IR neurons were also positive for ChAT-IR (Fig. 1F/F'), but a small population of D1-positive and ChAT-negative neurons were observed (white arrows); and (III) D2 had a similar distribution pattern to that of D1 in the HN (data not shown).

3.2. Characterization of the 6-OHDA-induced PD rat model

TH-IR neurons in the SN are dopaminergic. Six weeks after injecting 6-OHDA into the SN, western blot analysis revealed that the protein level of TH in the SN was significantly decreased, from 0.59 ± 0.08 to 0.21 ± 0.06 (Fig. 2A, $n = 6$, $P < 0.001$). On the 5th week after the bilateral injection of 6-OHDA into the SN, no significant difference was observed in food intake between the groups (Fig. 2B; control group, 20.5 ± 2.2 g; 6-OHDA group, 19.3 ± 2.3 g; $n = 12$, $P > 0.05$), but the daily food residue was significantly increased in the 6-OHDA group (Fig. 2C; control group, 1.26 ± 0.15 g; 6-OHDA group, 3.31 ± 0.26 g; $n = 12$, $P < 0.001$). A successful PD model should also present a disturbance in motor coordination. A rota-rod treadmill was used to evaluate the motor coordination of the rats. Rats with SN lesions exhibited a decreased treadmill occupancy time compared to that of the control group (Fig. 2D; control group, 88.9 ± 7.12 s; 6-OHDA group, 54.07 ± 6.44 s; $n = 6$, $P < 0.001$). In Fig. 2E, Nissl staining indicates the location of the HN, ventrolateral to the central canal (CC) and ventral to the dorsal motor nucleus of the vagus (DMV). No obvious gross morphological differences were observed between the control and 6-OHDA groups ($n = 6$).

3.3. Alteration of TH, ChAT, D1 and D2 mRNA expression in the HN of 6-OHDA rats

The relative levels of mRNA encoding TH, ChAT, D1 and D2 were normalized to that of β-actin. The mRNA expression levels in the HN were compared between control and 6-OHDA rats (Fig. 3A). No significant differences were found for TH and D1 (Fig. 3A/C, $n = 6$, $P > 0.05$), but decreased ChAT and increased D2 mRNA expression was observed in 6-OHDA rats. ChAT decreased from 0.97 ± 0.06 in the control group to 0.71 ± 0.10 in the 6-OHDA

Table 3
Sequences of primers.

Primers	GenBank accession numbers	Primer sequence	Primer location in sequence
TH	NM012740	Forward, 5′-AGTACAAGCACGGTGAACCA-3′	649–668
		Reverse, 5′-GGTCAGCCAACATGGGTACA-3′	1038–1019
ChAT	NM001170593	Forward, 5′-TGACAAGTCCCTGCAGTTCG-3′	1273–1292
		Reverse, 5′-CGAGATGGCCTTGGGTTTCT-3′	1493–1474
D1	NM012546	Forward, 5′-TGAGCCTTACAGCAGGAGTG-3′	1792–1811
		Reverse, 5′-AGCCACCACATCAGTCTTTG-3′	2070–2051
D2	NM012547	Forward, 5′-TTGCCATTGTTCTCGGTGTGT-3′	1473–1493
		Reverse, 5′-CCACAGCTTGCAGGGATGAG-3′	1759–1740
β-Actin	NM031144	Forward, 5′-CACCCGCGAGTACAACCTTC-3′	18–37
		Reverse, 5′-CCCATACCCACCATCACACC-3′	224–205

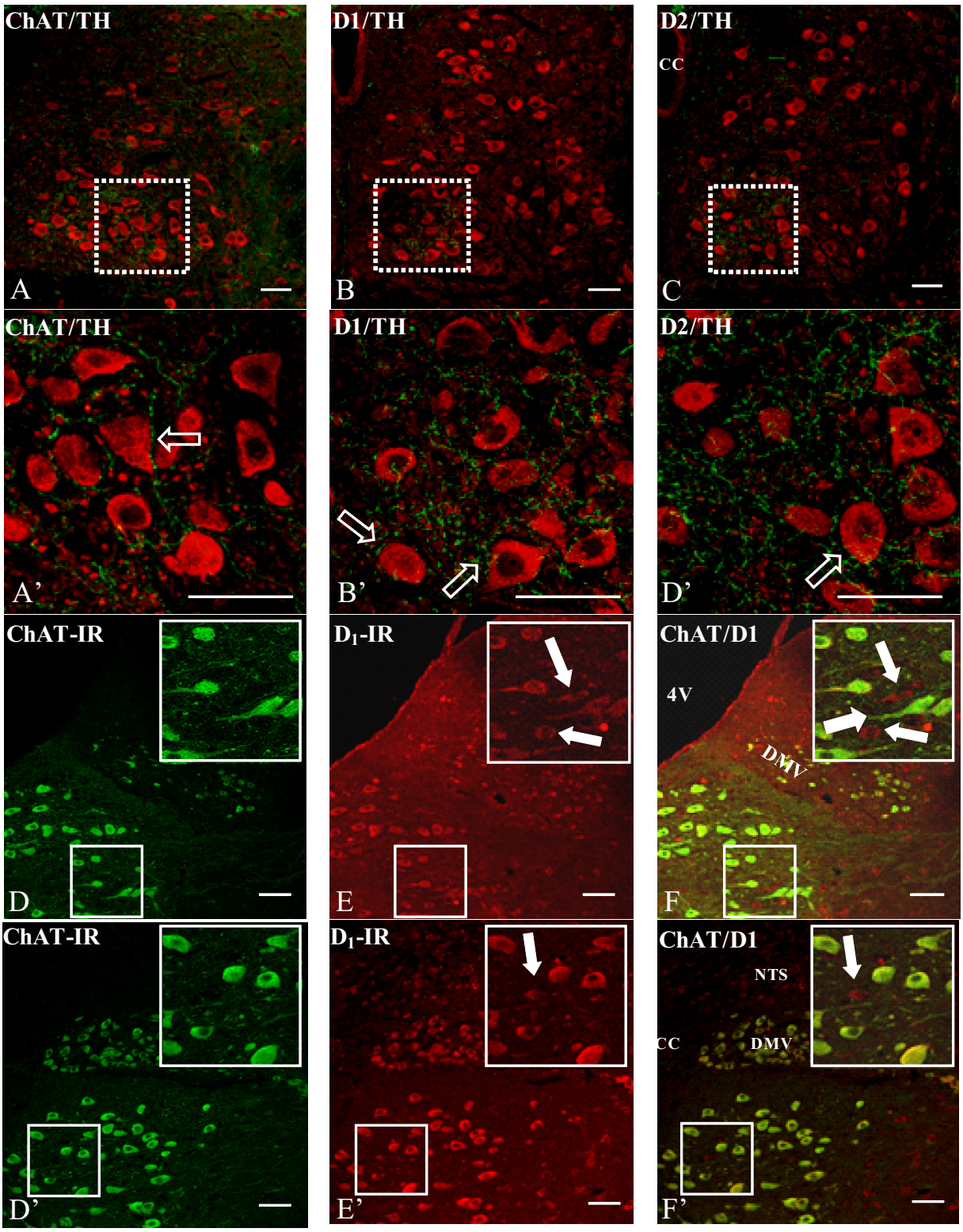

Fig. 1. Distribution of TH, ChAT, D1 and D2 in the HN of control rat. Double-label immunofluorescence of confocal z-stack images reveals the distribution of TH (A–C, green) with that of ChAT (A), D1 (B) and D2 (C) (red). Panels A–C are low-magnification images, whereas A'–C' are the high-magnification images of the respective boxed regions in A–C. The "empty arrows" point to the focal clustering of predominately TH-IR varicosities around ChAT, D1 or D2 immunoreactive perikarya. Double-label immunofluorescence of D1 and ChAT is shown at the rostral (B–D) and caudal (B'–D') levels of the HN. Each white dashed frame is magnified in the upper right corner. The "white arrows" indicate the immunofluorescence for D1-positive but ChAT-negative perikarya in the HN. NTS, nucleus of the solitary tract; DMV, dorsal motor nucleus of the vagus; CC, central canal; 4V, fourth ventricle. Scale bar: 50 μm. (For interpretation of the references to color in this figure legend, the reader is referred to the web version of this article.)

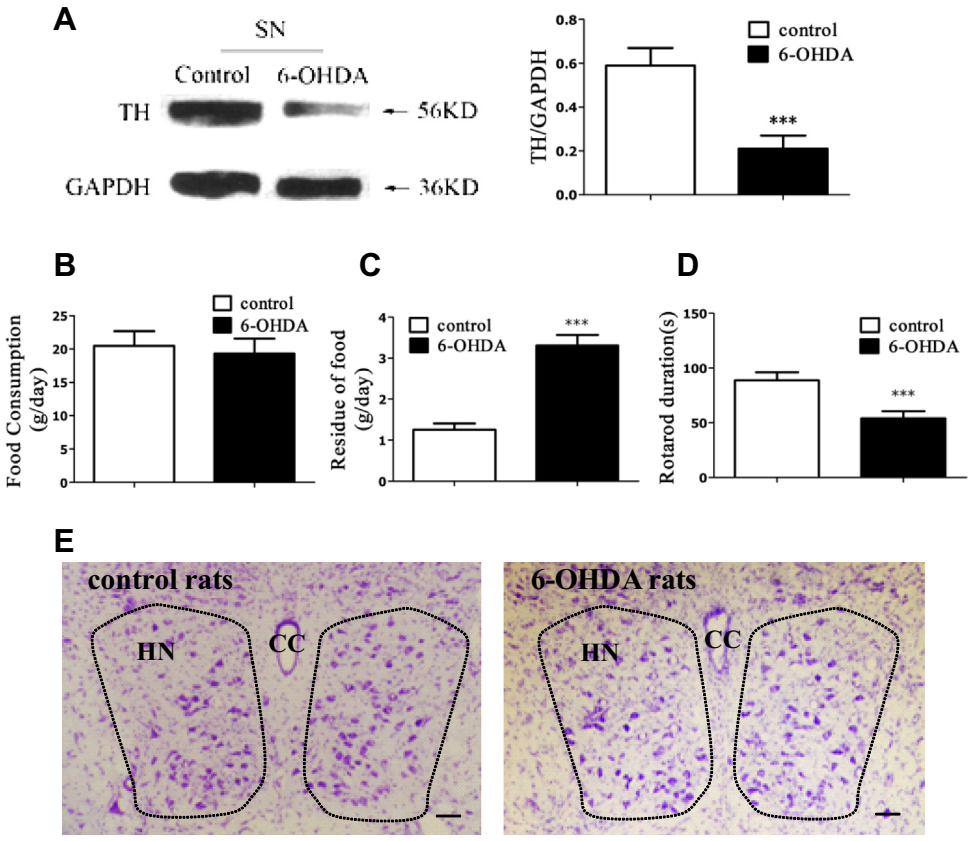

Fig. 2. Characterization of 6-hydroxydopamine (6-OHDA) rats. Representative Western blot for TH in the SN of control and 6-OHDA rats (A); GAPDH was analyzed as a loading control. The summary histogram indicates that TH protein expression in the SN was significantly decreased in 6-OHDA rats, $^{***}P < 0.001$. Daily food consumption is displayed as grams of dry food consumed per day during week 5 (B). The summary histogram indicates that the food residue was significantly increased in 6-OHDA rats (C), $^{***}P < 0.001$. 6-OHDA rats exhibited a decrease in the time spent on the rota-rod (D), $^{***}P < 0.001$. Nissl staining fails to reveal any gross morphological differences in the HN between control and 6-OHDA rats; the area enclosed by the dotted line depicts the boundaries of the HN (E). CC, central canal; Scale bar: 50 μm.

group, and D2 increased from 1.10 ± 0.11 in the control group to 1.45 ± 0.11 in the 6-OHDA group (Fig. 3A/C; $n = 6$, $P < 0.01$).

3.4. Alterations in TH, ChAT, D1 and D2 protein expression in the HN of 6-OHDA rats

Western blot analysis revealed an increase in the level of TH protein, from 0.22 ± 0.08 to 0.55 ± 0.08 (Fig. 3B/C, $n = 6$, $P < 0.001$), as well as a significant decrease in the level of ChAT protein, from 0.60 ± 0.05 to 0.28 ± 0.05 (Fig. 3B/C, $n = 6$, $P < 0.001$), in the 6-OHDA rats. A slight decrease in the level of D1 protein, from 0.71 ± 0.05 to 0.61 ± 0.05 (Fig. 3B/C, $n = 6$, $P < 0.01$), and an increase in the level of D2 protein, from 0.28 ± 0.05 to 0.35 ± 0.04 (Fig. 3B/C, $n = 6$, $P < 0.01$), was observed in the HN of 6-OHDA rats. In the ventromedial part of the HN (Fig. 3D, $n = 4$), the levels of TH-IR and D2-IR were higher in the 6-OHDA group than in the control group, whereas the inverse relationship was observed for ChAT-IR and D1-IR.

4. Discussion

The present study investigates the distribution of TH, ChAT, D1 and D2 in the HN of control and 6-OHDA rats using double-label immunofluorescence, Western blotting and SqRT–PCR. The principal findings include the following: (I) both dopamine receptors D1 and D2 were widely distributed in the HN and predominantly located in the ChAT-IR motoneurons; (II) TH-IR fibers and processes innervated the HN and exhibited close perisomatic contact with ChAT-IR, D1-IR or D2-IR neuron somas, suggesting a potent dopaminergic influence on the cholinergic motoneurons that express D1 and D2 in the HN; and (III) 6-OHDA rats (PD model) exhibited up-regulated TH and D2 expression and down-regulated ChAT and D1 expression in the HN. Furthermore, the 6-OHDA rats also displayed certain characteristics of PD, such as increased food residue and decreased treadmill occupancy time.

It has been reported that the HN receives catecholamine innervation [8,20], but immunohistochemical evidence for catecholaminergic innervation of HN motoneurons is lacking. In the present study, we demonstrated that dopamine receptors (D1 and D2) were mostly present in the ChAT-IR motoneurons in the HN and that TH-IR fibers with cluster varicosities were widely distributed around the motoneurons in the HN. Some of these fibers were observed in close proximity to the ChAT-IR, D1-IR and D2-IR motoneuron somas, suggesting that the function of ChAT-IR motoneurons in the HN might be regulated by dopaminergic innervation. Studies have found that genioglossal motoneurons participate in sucking, respiration, deglutition and mastication via tongue protrusion [21]. The present findings provide experimental evidence that genioglossal motoneurons are regulated by the dopaminergic system. TH-IR fibers in the HN have been reported to derive from noradrenergic nuclei such as the A5, sub-coeruleus, A1/C1 and A7 groups [20]. No direct innervation of dopaminergic fibers in the HN has been reported. However, a moderate DA level has been detected by in vivo microdialysis in the HN [9]. Additionally, the dialysate DA has also been measured in the primary motor and cerebellar cortices, which receive noradrenergic projections by only minor or no dopaminergic projections [22]. According to the study by McMill et al. in addition to the degeneration of dopaminergic

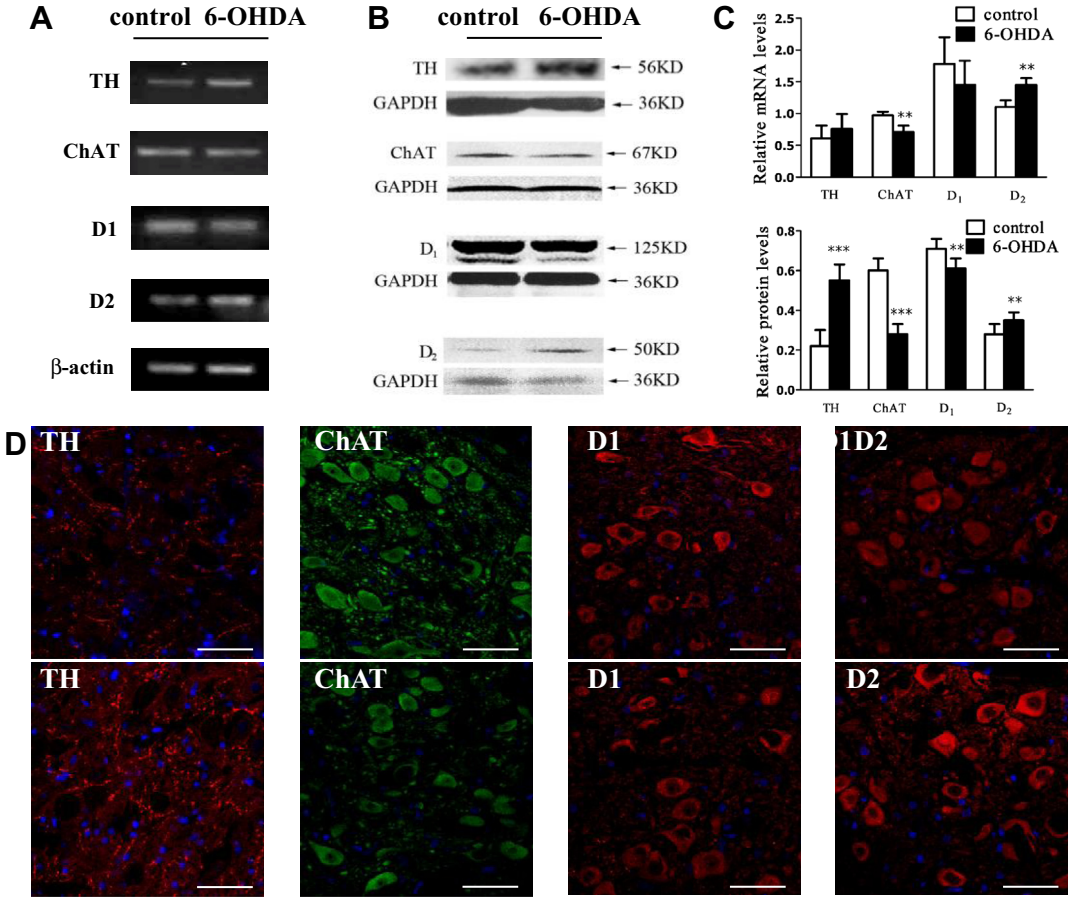

Fig. 3. TH, ChAT, D1 and D2 mRNA and protein expressions in the HN of control and 6-OHDA rats. Reverse transcription PCR revealed TH, ChAT, D1 and D2 expression in the HN of control and 6-OHDA rats (A). β-Actin was analyzed as a loading control. The summary histogram indicates that ChAT expression in the HN is significantly decreased, but the expression of D2 is increased in 6-OHDA rats compared to controls (C, upper), $^{**}P < 0.01$. Western blotting revealed TH, ChAT, D1 and D2 expression in the HN of control and 6-OHDA rats (B). GAPDH was analyzed as a loading control. The summary histogram of the western blots indicates that the expression of TH and D2 was increased, but that of ChAT and D1 was significantly decreased in the HN of 6-OHDA rats (C, lower). $^{**}P < 0.01$, $^{***}P < 0.001$. Representative confocal images revealed a similar trend for TH, ChAT, D1 and D2 alterations in the ventromedial HN of 6-OHDA rats. Scale bar: 50 μm.

neurons in the SN, loss of noradrenergic neurons occurs in the locus coeruleus, but not in other noradrenergic groups, such as the A1, A5 and A7, in PD patients [23]. In the present study, the enhanced TH expression in the HN after the destruction of dopaminergic neurons in the SN could be explained by a compensatory mechanism: the SN lesion may have induced the sprouting of TH terminals in the HN as an adaptation to the SN damage in 6-OHDA rats. To our knowledge, this is the first study to find expression of D1/D2 in cholinergic motoneurons, TH-IR fibers in close proximity to motoneuron somas and alterations in ChAT-IR, D1-IR, D2-IR and TH-IR in the HN of 6-OHDA rats. We have previously reported that the DMV serves to deliver altered CNS information to the gastric wall and causes gastric dysmotility in 6-OHDA rats [16]. Similarly, alterations in TH, ChAT, D1 and D2 in the HN might also play a role in impaired tongue motility in 6-OHDA rats.

Patients with PD have been shown to have reduced ChAT levels in all brain areas, with levels at 51% of the control mean in the hippocampus, 57% in the prefrontal cortex and 64% in the temporal cortex [24]. Consistent with these previous findings, the present study also found that ChAT expression in the HN was significantly reduced in 6-OHDA rats and that 6-OHDA rats exhibited a decreased number of motoneurons in the HN [25]. This deficit may be related to the impaired lingual functions observed in patients with PD [2–5]. Interestingly, the adjacent DMV also showed a similar trend with respect to TH and ChAT expression in 6-OHDA PD rats [26].

It is well known that the motoneurons in the HN of the medulla oblongata share an analogous motor pathway and function with the motoneurons in the ventral horn of the spinal cord. Allen et al. reported the colocalization of dopamine receptors D1- and D2-IR with ChAT-IR in the ventral cord motoneurons [27], which is consistent with the findings of the present study in the HN. D1 and D2 are classic subtypes of the dopamine receptor family. Activation of D1 may stimulate acetylcholine (ACh) release from cholinergic motoneurons via activation of the cyclic adenosine monophosphate (cAMP) pathway, whereas activation of D2 inhibits its ACh release via suppression of the cAMP pathway [28,29]. Therefore, coexpressed D1 and D2 in HN motoneurons might act antagonistically to modulate ACh release and thereby modulate tongue motility.

In conclusion, the cholinergic motoneurons in the HN express dopamine receptors and receive catecholaminergic innervation. The up-regulation of TH and D2 and down-regulation of D1 and ChAT may lead to a decrease in ACh release, which could be one of the mechanisms underlying dysphagia in PD patients.

Acknowledgments

This work was supported financially by Grants from the National Natural Science Foundation of China (81170346 and 81370482, J.X. Zhu; 31200897, Z.Y. Wang), the Beijing Natural Science Foundation (7121003 and 7132017 J.X. Zhu), the Project

of Construction of Innovative Teams and Teacher Career Development for University and Colleges under Beijing Municipality (IDHT20140514) and the Scientific Research Fund of Xinxiang Medical University (2013QN104, L. Zhou).

References

[1] A. Melo, L. Monteiro, Swallowing improvement after levodopa treatment in idiopathic Parkinson's disease: lack of evidence. Authors' reply, Parkinsonism Relat. Disord. 20 (2014) 342.
[2] R.F. Pfeiffer, I. Bodis-Wollner, Parkinson's Disease and Nonmotor Dysfunction, Humana Press, 2012.
[3] C.J. Hunker, J.H. Abbs, Uniform frequency of parkinsonian resting tremor in the lips, jaw, tongue, and index finger, Mov. Disord. 5 (1990) 71–77.
[4] N.P. Solomon, D.A. Robin, Perceptions of effort during handgrip and tongue elevation in Parkinson's disease, Parkinsonism Relat. Disord. 11 (2005) 353–361.
[5] N.A. Leopold, M.C. Kagel, Prepharyngeal dysphagia in Parkinson's disease, Dysphagia 11 (1996) 14–22.
[6] M.R. Ciucci, J.A. Russell, A.J. Schaser, E.J. Doll, L.M. Vinney, N.P. Connor, Tongue force and timing deficits in a rat model of Parkinson disease, Behav. Brain Res. 222 (2011) 315–320.
[7] A.L. Nuckolls, C. Worley, C. Leto, H. Zhang, J.K. Morris, J.A. Stanford, Tongue force and tongue motility are differently affected by unilateral vs bilateral nigrostriatal dopamine depletion in rats, Behav. Brain Res. 234 (2012) 343–348.
[8] L.D. Aldes, R.C. Chronister, L.A. Marco, J.W. Haycock, J. Thibault, Differential distribution of biogenic amines in the hypoglossal nucleus of the rat, Exp. Brain Res. 73 (1988) 305–314.
[9] Y.Y. Lai, T. Kodama, J.M. Siegel, Changes in monoamine release in the ventral horn and hypoglossal nucleus linked to pontine inhibition of muscle tone: an in vivo microdialysis study, J. Neurosci. 21 (2001) 7384–7391.
[10] A. Maqbool, T.F. Batten, P.A. Berry, P.N. McWilliam, Distribution of dopamine-containing neurons and fibres in the feline medulla oblongata: a comparative study using catecholamine-synthesizing enzyme and dopamine immunohistochemistry, Neuroscience 53 (1993) 717–733.
[11] M. Connaughton, J.V. Priestley, M.V. Sofroniew, F. Eckenstein, A.C. Cuello, Inputs to motoneurones in the hypoglossal nucleus of the rat: light and electron microscopic immunocytochemistry for choline acetyltransferase, substance P and enkephalins using monoclonal antibodies, Neuroscience 17 (1986) 205–224.
[12] I. Pose, S. Fung, S. Sampogna, M.H. Chase, F.R. Morales, Nitrergic innervation of trigeminal and hypoglossal motoneurons in the cat, Brain Res. 1041 (2005) 29–37.
[13] M. Kalia, K. Fuxe, M. Goldstein, Rat medulla oblongata. II. Dopaminergic, noradrenergic (A1 and A2) and adrenergic neurons, nerve fibers, and presumptive terminal processes, J. Comp. Neurol. 233 (1985) 308–332.
[14] N.E. Lazarov, U. Schmidt, I. Wanner, C. Pilgrim, Mapping of D1 dopamine receptor mRNA by non-radioactive in situ hybridization, Histochem. Cell Biol. 109 (1998) 271–279.
[15] T.M. Hyde, M.B. Knable, A.M. Murray, Distribution of dopamine D1–D4 receptor subtypes in human dorsal vagal complex, Synapse 24 (1996) 224–232.
[16] L.F. Zheng, J. Song, R.F. Fan, C.L. Chen, Q.Z. Ren, X.L. Zhang, X.Y. Feng, Y. Zhang, L.S. Li, J.X. Zhu, The role of the vagal pathway and gastric dopamine in the gastroparesis of rats after a 6-hydroxydopamine microinjection in the substantia nigra, Acta Physiol. (Oxf.) 211 (2014) 434–446.
[17] Y.M. Tian, X. Chen, D.Z. Luo, X.H. Zhang, H. Xue, L.F. Zheng, N. Yang, X.M. Wang, J.X. Zhu, Alteration of dopaminergic markers in gastrointestinal tract of different rodent models of Parkinson's disease, Neuroscience 153 (2008) 634–644.
[18] Q.Q. Cai, L.F. Zheng, R.F. Fan, H. Lian, L. Zhou, H.Y. Song, Y.Y. Tang, X.Y. Feng, Z.K. Guo, Z.Y. Wang, J.X. Zhu, Distribution of dopamine receptors D1- and D2-immunoreactive neurons in the dorsal motor nucleus of vagus in rats, Auton. Neurosci. 176 (2013) 48–53.
[19] W. Yu, Dissection of motor nuclei of trigeminal, facial, and hypoglossal nerves from fresh rat brain, in: A Dissection and Tissue Culture Manual of the Nervous System, Wiley-Liss, 1989, pp. 30–39.
[20] I. Rukhadze, L. Kubin, Differential pontomedullary catecholaminergic projections to hypoglossal motor nucleus and viscerosensory nucleus of the solitary tract, J. Chem. Neuroanat. 33 (2007) 23–33.
[21] E.F. Bailey, A.D. Rice, A.J. Fuglevand, Firing patterns of human genioglossus motor units during voluntary tongue movement, J. Neurophysiol. 97 (2007) 933–936.
[22] P. Devoto, G. Flore, L. Pani, G.L. Gessa, Evidence for co-release of noradrenaline and dopamine from noradrenergic neurons in the cerebral cortex, Mol. Psychiatry 6 (2001) 657–664.
[23] P.J. McMillan, S.S. White, A. Franklin, J.L. Greenup, J.B. Leverenz, M.A. Raskind, P. Szot, Differential response of the central noradrenergic nervous system to the loss of locus coeruleus neurons in Parkinson's disease and Alzheimer's disease, Brain Res. 1373 (2011) 240–252.
[24] P.M. Mattila, M. Roytta, P. Lonnberg, P. Marjamaki, H. Helenius, J.O. Rinne, Choline acetyltransferase activity and striatal dopamine receptors in Parkinson's disease in relation to cognitive impairment, Acta Neuropathol. 102 (2001) 160–166.
[25] M.J. Eadie, The pathology of certain medullary nuclei in Parkinsonism, Brain 86 (1963) 781–792.
[26] L.F. Zheng, Z.Y. Wang, X.F. Li, J. Song, F. Hong, H. Lian, Q. Wang, X.Y. Feng, Y.Y. Tang, Y. Zhang, J.X. Zhu, Reduced expression of choline acetyltransferase in vagal motoneurons and gastric motor dysfunction in a 6-OHDA rat model of Parkinson's disease, Brain Res. 1420 (2011) 59–67.
[27] A.T. Allen, K.N. Maher, K.A. Wani, K.E. Betts, D.L. Chase, Coexpressed D1- and D2-like dopamine receptors antagonistically modulate acetylcholine release in *Caenorhabditis elegans*, Genetics 188 (2011) 579–590.
[28] P.B. Schwarz, J.H. Peever, Dopamine triggers skeletal muscle tone by activating D1-like receptors on somatic motoneurons, J. Neurophysiol. 106 (2011) 1299–1309.
[29] R.J. Baldessarini, F.I. Tarazi, Brain dopamine receptors: a primer on their current status, basic and clinical, Harv. Rev. Psychiatry 3 (1996) 301–325.